



## Mitigation of PM<sub>2.5</sub> and Ozone Pollution in Delhi: A Sensitivity Study during the Pre-monsoon period

Ying Chen<sup>1,2\*</sup>, Oliver Wild<sup>1,2</sup>, Edmund Ryan<sup>1,9</sup>, Saroj Kumar Sahu<sup>4</sup>, Douglas Lowe<sup>5</sup>, Scott  
Archer-Nicholls<sup>6</sup>, Yu Wang<sup>5</sup>, Gordon McFiggans<sup>5</sup>, Tabish Ansari<sup>1</sup>, Vikas Singh<sup>7</sup>, Ranjeet S.

5 Sokhi<sup>8</sup>, Alex Archibald<sup>6</sup>, Gufran Beig<sup>3</sup>

<sup>1</sup>Lancaster Environment Centre, Lancaster University, Lancaster, LA1 4YQ, UK

<sup>2</sup>Data Science Institute, Lancaster University, Lancaster, LA1 4YW, UK

<sup>3</sup>Indian Institute of Tropical Meteorology, Pune, India

<sup>4</sup>Environmental Science, Dept. of Botany, Utkal University, Bhubaneswar, India

10 <sup>5</sup>Centre for Atmospheric Sciences, School of Earth, Atmospheric and Environmental Sciences,  
University of Manchester, Manchester, UK

<sup>6</sup>NCAS-Climate, Department of Chemistry, University of Cambridge, Cambridge, UK

<sup>7</sup>National Atmospheric Research Laboratory, Gadanki, AP, India

15 <sup>8</sup>Centre for Atmospheric and Climate Physics Research, University of Hertfordshire, Hatfield,  
Hertfordshire, UK

<sup>9</sup>School of Mathematics, University of Manchester, Manchester, UK

*Correspondence to: Ying Chen (y.chen65@lancaster.ac.uk)*



**Abstract:**

Fine particulate matter ( $PM_{2.5}$ ) and surface ozone ( $O_3$ ) are major air pollutants in megacities such as Delhi, but the design of suitable mitigation strategies is challenging. Some strategies for reducing  $PM_{2.5}$  may have the notable side-effect of increasing  $O_3$ . Here, we demonstrate a numerical framework for

25 investigating the impacts of mitigation strategies on both  $PM_{2.5}$  and  $O_3$  in Delhi. We use Gaussian process emulation to generate a computationally efficient surrogate for a regional air quality model (WRF-Chem). This allows us to perform global sensitivity analysis to identify the major sources of air pollution, and to generate emission-sector based pollutant response surfaces to inform mitigation policy development. Based on more than 100,000 emulation runs during the pre-monsoon period (peak  $O_3$  season), our global

30 sensitivity analysis shows that local traffic emissions from Delhi city region and regional transport of pollutions emitted from the National Capital Region surrounding Delhi (NCR) are dominant factors influencing  $PM_{2.5}$  and  $O_3$  in Delhi. They together govern the  $O_3$  peak and  $PM_{2.5}$  concentration during daytime. Regional transport contributes about 80% of the  $PM_{2.5}$  variation during the night. Reducing traffic emissions in Delhi alone (e.g., by 50%) would reduce  $PM_{2.5}$  by 15-20% but lead to a 20-25%

35 increase in  $O_3$ . However, we show that reducing NCR regional emissions by 25-30% at the same time would further reduce  $PM_{2.5}$  by 5-10% in Delhi and avoid the  $O_3$  increase. This study provides scientific evidence to support the need for joint coordination of controls on local and regional scales to achieve effective reduction on  $PM_{2.5}$  whilst minimize the risk of  $O_3$  increase in Delhi.



## 1. Introduction

40 Exposure to air pollutants increases morbidity and mortality (Huang et al., 2018a;WHO, 2013). The urban air quality in India, especially in Delhi, is currently among the poorest in the world (WHO, 2013, 2016b, a). In addition to the local impacts, the Indian monsoon can transport air pollutants to remote oceanic regions, inject them into the stratosphere and redistribute them globally (Lelieveld et al., 2018). This makes the impact of Indian air pollution wide ranging regionally and globally as well as having  
45 interactions with climate and ecosystems world-wide.

PM<sub>2.5</sub> (particulate matter with an aerodynamic diameter of less than 2.5 μm) is a major air pollutant, causing increases in disease (Pope et al., 2009;Gao et al., 2015;Stafoggia et al., 2019) and reduced visibility (Mukherjee and Toohey, 2016;Wang and Chen, 2019;Khare et al., 2018). The population of India experiences high PM<sub>2.5</sub> exposure, and this is responsible for ~1 million premature deaths per year  
50 (Conibear et al., 2018;Gao et al., 2018). Residential emissions are estimated to contribute ~50% of PM<sub>2.5</sub> concentrations and to cause more than 0.5 million annual mortalities across India (Conibear et al., 2018). The World Health Organization (WHO) reported an annual averaged PM<sub>2.5</sub> loading of ~140 μg/m<sup>3</sup> in Delhi in 2016 (WHO, 2016b), leading to ~11,000 premature deaths per year in the city (Chowdhury and Dey, 2016). In Delhi, the traffic sector (~50%) and the domestic sector (~20%) are the major local  
55 contributors to PM<sub>2.5</sub> (Marrapu et al., 2014). Efforts to control traffic emissions in Delhi in recent years by introducing an alternating ‘odd-even’ licence plate policy have led to reductions in PM<sub>2.5</sub> of less than 10% (Chowdhury et al., 2017). This indicates that there is an urgent need for a coordinated plan to mitigate PM<sub>2.5</sub> pollution (Chowdhury et al., 2017).

Surface ozone (O<sub>3</sub>), another major air pollutant, is damaging to health and reduces crop yields  
60 (Ashworth et al., 2013;Lu et al., 2018;Kumar et al., 2018). The risks of respiratory and cardiovascular diseases are increased from short-term exposure to high ambient O<sub>3</sub> and from long-term exposure at low levels (WHO, 2013;Turner et al., 2016;Fleming et al., 2018). Oxidation of volatile organic compounds (VOCs) in the presence of nitrogen oxides (NO<sub>x</sub>) is the main source of surface ozone. Rapid economic development in India has greatly increased the emissions of these O<sub>3</sub> precursors (Duncan et al., 2016),



65 leading to significant increases in  $O_3$  especially during the pre-monsoon period (Ghude et al., 2008). Hourly maximum  $O_3$  reaches as much as 140 ppbv during the pre-monsoon season in Delhi (Ghude et al., 2008), comparable to the most polluted regions in China (150 ppbv, Wang et al., 2017) and higher than the most polluted areas in the U.S. (110 ppbv, Lu et al., 2018).

Mitigation of  $PM_{2.5}$  pollution may lead to an increase in surface ozone, because the dimming effect  
70 of aerosols and removal of hydroperoxy radicals are reduced, facilitating  $O_3$  production (Huang et al., 2018b; Li et al., 2018; Hollaway et al., 2019). Furthermore, co-reduction of  $NO_x$  and  $PM_{2.5}$  emissions may increase  $O_3$  in cities where  $O_3$  production is in a VOC-limited photochemical regime (Ran et al., 2009; Xing et al., 2018; Xing et al., 2017). This has recently been reported in a number of Asian megacities, e.g. Shanghai (Ran et al., 2009), Beijing (Wu et al., 2015; Liu et al., 2017; Chen et al., 2018a) and  
75 Guangzhou (Liu et al., 2013). Delhi and coastal cities in India, which are known to be VOC-limited (Sharma et al., 2017), may face increased  $O_3$  as a side-effect of emission controls focused on  $PM_{2.5}$ . Therefore, studies of mitigation strategies that target both  $PM_{2.5}$  and  $O_3$  are urgently needed (Chen et al., 2018a), particularly as urban air pollution in India has been much less well studied than in many other countries.

80 To investigate the impacts of mitigation strategies with respect to both  $PM_{2.5}$  and  $O_3$ , we demonstrate a framework for generating emission-sector based pollutant response surfaces using Gaussian process emulation (O'Hagan and West, 2009; O'Hagan, 2006). We conduct global sensitivity analysis to identify the dominant emission sectors controlling  $PM_{2.5}$  and  $O_3$ , and then generate sector based response surfaces to quantify the impacts on  $PM_{2.5}$  and  $O_3$  of emission reductions. In contrast to simple sensitivity analysis  
85 varying one input at a time, this allows full exploration of the entire input space, accounting for the interactions between different inputs (Pisoni et al., 2018; Saltelli et al., 1999). Conventionally, chemical transport models (CTMs, e.g. WRF-Chem) are used to calculate the impacts on pollutants concentrations of different mitigation scenarios. However, the computational expensive of CTMs makes them unsuitable for performing global sensitivity analysis or generating response surfaces, which usually require  
90 thousands of model runs. To overcome this difficulty, source-receptor relationships (Amann et al., 2011)



or computational efficient surrogate models, trained on a limited number of CTM simulations, are used to replace the expensive CTM. These approaches have been used to perform sensitivity and uncertainty analysis of regional air quality models (Pisoni et al., 2018), assessment of regional air quality plans (Zhao et al., 2017; Xing et al., 2017; Pisoni et al., 2017; Thunis et al., 2016) and sensitivity and uncertainty  
95 analysis of global and climate simulations (Ryan et al., 2018; Lee et al., 2016; Lee et al., 2012). Here, we use surrogate model to explore the sensitivity of  $PM_{2.5}$  and  $O_3$  on sector based emission controls in Delhi, for developing a mitigation strategy addressing both pollutants.

In this study, we demonstrate the value of such a framework for supporting decision makers in determining better mitigation strategies. We give examples of its use in investigating impacts of  
100 mitigation scenarios on  $PM_{2.5}$  and  $O_3$  pollutions in Delhi, and demonstrate that regional joint coordination of emission controls over National Capital Region (NCR) of Delhi is essential for an effective reduction of  $PM_{2.5}$  whilst minimizing the risk of  $O_3$  increase.

## 2. Materials and Methods

### 105 2.1 WRF-Chem Model Baseline Simulation

WRF-Chem (v3.9.1) – an online, fully coupled chemistry transport model (Grell et al., 2005) – has been widely used in previous studies of air quality across India (Marrapu et al., 2014; Mohan and Gupta, 2018; Gupta and Mohan, 2015; Mohan and Bhati, 2011). The model has also been used to estimate the health burden (Conibear et al., 2018; Ghude et al., 2016) and reduction in crop yields (Ghude et al., 2014)  
110 from the exposure to  $PM_{2.5}$  and  $O_3$  over India.

In this study, we focus on the hot and dry pre-monsoon period in Delhi, when average temperatures are around 32 °C and relative humidity (RH) is about 35% (Ojha et al., 2012).  $O_3$  approaches its annual peak in pre-monsoon due to strong solar radiation (Ghude et al., 2008; Ojha et al., 2012). During the pre-monsoon period, desert dust can contribute significantly to particulate matter in Delhi (Kumar et al.,



115 2014b;Kumar et al., 2014a). Here, we perform WRF-Chem simulation for the period of 2–15 May 2015  
(with two additional days for spin-up), which was not significantly influenced by dust storm in Delhi  
according to MODIS observations (<https://earthdata.nasa.gov/earth-observation-data/near-real-time/hazards-and-disasters/dust-storms>). Strong dust storms started to influence the Indo Gangetic Plain  
on 21–24 April and 19 May 2015, respectively. This minimizes the uncertainties resulting from dust storm  
120 simulation and permits a stronger focus on anthropogenic emissions. Resuspended dust from road traffic  
is also a major contributor to PM<sub>2.5</sub> in Delhi, and this is estimated and included in the emission inventory  
as described below.

The model configuration follows the study of Marrapu et al. (2014), and the parameterizations used  
are listed in Table 1. Three nested domains are used, with coverage of South Asia (45 km resolution), the  
125 Indo Gangetic Plain (15 km resolution), and the National Capital Region (5 km resolution), see Fig. 1. A  
test simulation with a fourth domain over Delhi at 1.67 km resolution suggests that a further increase in  
resolution does not substantially improve model performance (details in Text S1), and this is in line with  
results from a previous study (Mohan and Bhati, 2011). The Carbon Bond Mechanism version Z (CBMZ,  
Zaveri and Peters, 1999) coupled with the MOSAIC (Zaveri et al., 2008) aerosol module with four size  
130 bins is used to represent gaseous chemical reaction and aerosol chemical and dynamical processes. We  
neglect wet scavenging and cloud chemistry processes here, as the impact of these is likely to be negligible  
during the dry pre-monsoon period over India.

The initial and boundary conditions for chemical species are provided from MOZART-4 global  
results (<https://www.acom.ucar.edu/wrf-chem/mozart.shtml>). Our baseline simulation is driven by  
135 European Centre for Medium-Range Weather Forecasts (ECMWF) meteorological data, as we find that  
this reproduces regional meteorology better than that from the National Centers for Environmental  
Prediction (NCEP) over India, consistent with a recent study (Chatani and Sharma, 2018). The wind  
pattern and temperature over Delhi in May 2015 is generally captured well in simulations driven by either  
meteorological dataset, but the model captures the variation in relative humidity much better ( $R=0.7$ ) with



140 ECMWF data than with NCEP data ( $R=0.4$ , negative bias of 20-40%). More detailed discussion is provided in Text S2.

The high-resolution Fire Inventory from NCAR (FINN, Wiedinmyer et al., 2011) is adopted to provide biomass burning emissions. Interactive biogenic emissions are included using the Model of Emissions of Gases and Aerosols from Nature (MEGAN, Guenther et al., 2006). The global Emission  
145 Database for Global Atmospheric Research with Task Force on Hemispheric Transport of Air Pollution (EDGAR-HTAP, Janssens-Maenhout et al., 2015) version 2.2 (year 2010) at  $0.1^\circ \times 0.1^\circ$  resolution is used to represent anthropogenic emissions apart from over Delhi, where they are represented by a high-resolution monthly inventory for 2015 developed under the System of Air Quality Forecasting and Research (SAFAR) project (Sahu et al., 2011; Sahu et al., 2015). In the absence of a diurnal variation in  
150 emissions specific to Delhi, we adopt diurnal variations from Europe in this study (Denier van der Gon et al., 2011). The SAFAR inventory provides emission fluxes of  $PM_{10}$ ,  $PM_{2.5}$ , black carbon, organic carbon,  $NO_x$ ,  $CO$ ,  $SO_2$  and NMVOC (non-methane volatile organic compounds) from five sectors, including power (POW), industry (IND), domestic or residential (DOM), traffic (TRA) and wind blow dust from roads (WBD). Wind blow dust includes dust resuspended from vehicle movement on paved  
155 and unpaved roads (Sahu et al., 2011), and is therefore closely related to traffic emissions, and we combine this into the traffic sector for our study.

The NMVOC emissions are speciated according to the EDGAR (v4.3.2) global inventory (Huang et al., 2017), and are then lumped for the CBMZ chemistry scheme. The speciation mapping is detailed in Table 2 and described below, and a toolkit has been developed to perform this mapping. Emissions of  
160 alcohols and ethers are split 20%:80% between methanol and ethanol by mass and then converted to molar emissions with a fractionation based on (Murrells et al., 2009). Emissions of paraffin carbon (PAR) are calculated by converting mass emissions from each VOC group to molar emissions and then multiplying by the number of paraffin carbons in order to conserve carbon. Hexanes and higher alkanes are converted to molar emissions of hexane and then multiplied by six to give PAR emissions. Other  
165 alkenes are mapped to molar emissions of butane, and this is then apportioned between terminal olefin



carbons (OLET), internal olefin carbons (OLEI) and PAR on a molar ratio of 1:1:4 following (Zaveri and Peters, 1999). Ketones are split 60%:40% by mass between acetone (KET) and methyl-ethyl ketone (MEK), then converted to molar emissions with fractions based on (Murrells et al., 2009). As MEK is not included in the CBMZ mechanism, we apportion molar emissions of MEK equally between KET and  
170 PAR.

## 2.2 Observational Network

Air quality and meteorological monitoring networks are operated in Delhi under the SAFAR project coordinated by IITM (Ministry of Earth Sciences, Government of India). Measurements of PM<sub>2.5</sub>, O<sub>3</sub> and NO<sub>x</sub> during the May 2015 simulation period are available from six monitoring stations in Delhi: C V  
175 Raman (CVR), Delhi University (DEU), Indira Gandhi International Airport Terminal-3 (AIR), Ayanagar (AYA), NCMRWF (NCM) and Pusa (PUS). The instruments are calibrated and measurements are quality controlled in the SAFAR project (<http://safar.tropmet.res.in>); more details are given in previous studies (Sahu et al., 2011;Beig et al., 2013;Aslam et al., 2017). Site locations are shown in Fig. 2 and measured variables are given in Table S1.

## 180 2.3 Global Sensitivity Analysis of Urban Air Pollution

We perform global sensitivity analysis (Iooss and Lemaître, 2015) to quantify the sensitivity of modelled PM<sub>2.5</sub> and O<sub>3</sub> to each emission sector. Global sensitivity analysis has major advantages over a simple one-at-a-time sensitivity analysis, where a single input is varied while the other inputs are fixed at nominal values, as the latter approach can lead to underestimation of the true sensitivity (Saltelli et al.,  
185 1999;Pisoni et al., 2018). The extended Fourier Amplitude Sensitivity Test (eFAST, Saltelli et al., 1999) is a commonly used approach to perform GSA, and is adopted in this study. Since eFAST typically requires thousands of model runs, we employ a computationally cheaper surrogate model in place of WRF-Chem. In this study, we use Gaussian process emulation to create the surrogate model (O'Hagan, 2006), since a Gaussian process emulator typically requires a relatively small number of runs of the  
190 computationally-expensive model to generate. This is in contrast to other surrogate modelling approaches, such as neural networks, which typically require thousands of model runs to train them. Gaussian process





emulators have been used previously in the uncertainty assessment of atmospheric models (Lee et al., 2016; Lee et al., 2012; Lee et al., 2011). Following these studies, a Latin hypercube space-filling approach is employed to provide the designs of training runs for WRF-Chem. Latin hypercube sampling is a statistical method for generating a near-random sample of parameter values from a multidimensional distribution (Shields and Zhang, 2016). Here, we search through 100,000 Latin hypercube random designs to find the optimal one where the parameter space is filled most effectively. More details of these approaches are described in a previous study (Ryan et al., 2018).

In this study, we focus on a limited number of the emission sectors to demonstrate the effectiveness of the approach: domestic/residential emissions in Delhi (DOM), traffic emissions in Delhi (TRA, including WBD), power and industry in Delhi (POW+IND) and total emissions in the National Capital Region outside Delhi (NCR). NCR represents the contribution of regional transport to pollution in Delhi. According to the SAFAR emission inventory, the total PM<sub>2.5</sub> emissions of DOM, TRA, POW+IND and NCR are about 1.8, 6.1, 3.1 and 8.5 Gg/month in May 2015, respectively. Gaussian process emulators are built based on 20 training runs of WRF-Chem, with emission scaling drawn from a variation range of 0-200% for each of the four specified sectors (Table S2). Emulation of the impacts of mitigation scenarios on PM<sub>2.5</sub> and O<sub>3</sub> can be performed in minutes on a laptop, in contrast to simulations with WRF-Chem which require a few days on a high-performance computing cluster. We perform ‘leave-one-out’ cross-validation (O’Hagan and West, 2009; Wang et al., 2011) with 10,000 random samples to check that the Gaussian process emulator can fully represent the results of WRF-Chem. Modelled and emulated O<sub>3</sub> and PM<sub>2.5</sub> lie very close to the 1:1 line with R values of more than 0.99 as shown in Fig. 3, suggesting that the emulation provides a good representation of the model.

## 2.4 Response Surfaces

Response surfaces are useful for investigating the relationship between model inputs and outputs, in this case between sectoral emissions and modelled pollutant concentrations. They have been widely applied for air quality studies and policy making (EPA, 2006a, b; Zhao et al., 2017; Xing et al., 2017). Here, we analyse the responses of PM<sub>2.5</sub> and O<sub>3</sub> to changes in emissions from each sector of between 0%



and 200%. The computationally efficient Gaussian process emulation enables us to generate response surfaces without the computational burden of a large number of runs of the WRF-chem model.

## 220 2.5 Outline of Analysis

We use the WRF-Chem model to simulate the hourly concentrations of O<sub>3</sub> and PM<sub>2.5</sub> over the Delhi region during 2-15 May 2015 and evaluate the results against observations. We perform a simple sensitivity analysis to investigate the contributions of biomass burning and biogenic emissions to PM<sub>2.5</sub> and O<sub>3</sub> in Delhi. We then conduct a global sensitivity analysis, using Gaussian process emulation, to  
225 determine the sensitivity of modelled O<sub>3</sub> and PM<sub>2.5</sub> concentrations to changes in the dominant anthropogenic emission sectors. Finally, we generate response surfaces to identify appropriate mitigation strategies for reducing PM<sub>2.5</sub> while minimizing the risks from O<sub>3</sub> increase.

## 3. Results and Discussion

### 230 3.1 Model Performance

The WRF-Chem model captures the general magnitude and variation in PM<sub>2.5</sub> well (Fig. 4a), with mean bias and error of about -3.5% and 11%, respectively, and an index of agreement (Willmott et al., 2012) of 75%. The frequency distributions of modelled PM<sub>2.5</sub> are also similar to the observations, with differences in mean and median concentrations of less than 10%, although high concentration spikes are  
235 missed by the model (Fig. S1). The modelled PM<sub>2.5</sub> peaks around 09:00 local time (LT) because the rush hour enhances traffic emissions before the planetary boundary layer (PBL) height has increased (Fig. 4a). This is also seen in the modelled results at DEU (Fig. S2), which is closer to a motorway and shows a more intense PM<sub>2.5</sub> peak in the morning rush hour. PM<sub>2.5</sub> is overestimated during the morning rush hour (around 09:00 am) and underestimated during the early morning (03:00-05:00 LT, Fig. 4a and Fig. S2).  
240 This may suggest that there is an earlier rush hour or more traffic activity at night in Delhi than in European cities, since we adopted European diurnal emission patterns in this study in the absence of local



information. Detailed studies of traffic emissions and their variation in Delhi would help improve these model simulations.

The modelled chemical composition of  $PM_{2.5}$  is shown in Fig. S3. Secondary inorganic aerosol (SIA),  
245 including sulphate, nitrate and ammonium, only contributes ~25% of aerosol mass in our simulation. In  
the absence of particle inorganic composition measurements during the simulation period, we compare  
our results with a previous modelling study of Delhi during the post-monsoon season (Marrapu et al.,  
2014), which also shows a ~25% contribution of SIA to  $PM_{2.5}$  loading, in line with our results.  
Furthermore, our results are also consistent with an observational study, which reported the mass fraction  
250 of organic matter (usually calculated as 1.4 times OC) and elemental carbon (usually equivalent to black  
carbon in modelling studies, (Chen et al., 2016b) in  $PM_{2.5}$  of ~20% and ~6% in Delhi during May 2015,  
respectively (Sharma et al., 2018).

The model well captures the peak  $O_3$  with a bias of less than 5%, although it underestimates  $O_3$   
during night-time (Fig. 4b). In general, the diurnal pattern and magnitude of  $O_3$  are captured by WRF-  
255 Chem (Fig. 4b), with normalized mean bias and error of about -20% and 35%, respectively, and an index  
of agreement of 65%. The underestimation during night-time is likely to be because  $NO_x$  is overestimated  
by a factor of 2-3 at night (Fig. S4), and the excess NO depletes  $O_3$ . This is indicated by the frequency  
distribution of  $O_3$  and  $NO_x$  (Fig. S5), where the median values of observed  $O_3$  and  $NO_x$  are matched well  
by the model. However, the higher peaks of modelled  $NO_x$  concentration lower the modelled  $O_3$  levels,  
260 indicating that Delhi is in VOC-limited photochemical regime. Similar results are found at AYA (Fig.  
S6). The larger underestimation of  $O_3$  at NCM (Fig. S5d, industrial environment site) suggests that  $NO_x$   
emission from the industry sector may be overestimated.

### 3.2 Impacts of Biogenic and Biomass Burning Emissions

Before exploring the importance of the four selected anthropogenic emission sectors on  $PM_{2.5}$  and  
265  $O_3$  in Delhi during simulation period, we investigate the contributions from other factors (biomass burning  
and biogenic emissions). We remove these sources and find that there is a negligible contribution from



biogenic emissions to  $PM_{2.5}$  concentrations over Delhi in this season (Fig. 4c and 4d). It is worth noting that biogenic emissions may contribute to secondary organic aerosol (SOA) in Delhi, but the formation of SOA is not well represented by the CBMZ-MOSAIC chemistry-aerosol mechanisms used in this study.

270 However, this weakness is not expected to have a major influence on our pre-monsoon results; as described before, the difference of organic matter fraction between simulation and observation (Sharma et al., 2018) in May 2015 is less than 5%. About 10% of  $PM_{2.5}$  in Delhi is derived from biomass burning during the simulation period. Crop burning in Haryana and Punjab states is a major source of this (Jethva et al., 2018; Cusworth et al., 2018). In contrast, there is a negligible contribution from biomass burning to

275  $O_3$ . However, there is a 15-20% contribution to  $O_3$  from biogenic emission of VOCs, highlighting that  $O_3$  production in Delhi is strongly VOC-limited.

### 3.3 Effect of the Diurnal Variation in Emissions

In order to investigate the competing influences of meteorology and human activities on the diurnal patterns of  $PM_{2.5}$  and  $O_3$  over Delhi, we test the effect of removing the diurnal variation in anthropogenic

280 emissions ('noDiurnal', see Fig. 4c and 4d). Modelled  $PM_{2.5}$  concentrations are very similar to the 'baseline' run during daytime when the PBL is well developed, with differences of less than 5%. This suggests that meteorological processes such as vertical mixing, advection and transport are the dominant factors controlling  $PM_{2.5}$  in the daytime. In contrast, freshly emitted pollutants are trapped at night when the PBL is shallow, and concentrations are very sensitive to the emission flux, so that the diurnal pattern

285 of emissions is the dominant factor at night. The  $PM_{2.5}$  concentration is almost doubled in the early morning (03:00-09:00 LT, Fig. 4c) when the PBL is shallow and emissions in the 'noDiurnal' case are higher. There is also a large increase in  $NO_x$  in the early morning (Fig. S4), which leads to greater depletion of  $O_3$  (Fig. 4d). However, the concentration of  $O_3$  is about 20-25% higher during the ozone peak hour in the afternoon in the 'noDiurnal' case, as the daytime  $NO_x$  emissions are less (Fig. S4). This

290 sensitivity test also highlights the VOC-limited nature of  $O_3$  production in Delhi.



### 3.4 Sensitivity Analysis of Pollutants in Delhi

The importance of each anthropogenic emission sector to pollutant concentrations in Delhi is investigated using global sensitivity analysis and indicated by global sensitivity indices (SIs), as shown in Fig. 5. The sensitivity index is a measure of the contribution of the variation in pollutants from one emission sector to the total variation across all four sectors considered here. A larger SI indicates a larger influence from the corresponding sector to the modelled average surface PM<sub>2.5</sub> or O<sub>3</sub> over Delhi City Region (marked in Fig. 2) in this study.

The PM<sub>2.5</sub> concentration is most sensitive to emissions from the NCR region surrounding Delhi, with a sensitivity index higher than 50% most of time (Fig. 5a) and reaching 80-90% and ~60% during 03:00-07:00 LT and 12:00-17:00 LT, respectively. During the rush hours in the morning and evening, the sensitivity to NCR emissions is lower, while the sensitivity to Delhi traffic emissions increases by ~30%. Around 10:00 LT, local traffic emissions and emissions from NCR have a similar effect on PM<sub>2.5</sub>. In contrast, local traffic emissions dominate the PM<sub>2.5</sub> in Delhi around 20:00 LT, with a sensitivity contribution of up to ~80%. This is caused by the collapse of the PBL in the evening rush hour at around 20:00 LT which enhances the sensitivity to fresh local emissions. Local traffic emissions contribute ~60% of primary PM<sub>2.5</sub> emission in Delhi (Fig. 6a), which remains concentrated in the PBL during rush hours. In contrast, the fully developed PBL in the daytime mixes air down from the free troposphere (Chen et al., 2016a), where regional transport of pollutants from NCR can be important. This could explain the second peak in the sensitivity to NCR emissions (50-60%) during the afternoon (Fig. 5a).

The O<sub>3</sub> in Delhi City Region is overwhelmingly dominated by local traffic emissions with a sensitivity index higher than 80% at night-time (Fig. 5b). Traffic contributes ~75% of total NO<sub>x</sub> emission in Delhi (Fig. 6b), and the shallow PBL during the night traps the NO<sub>x</sub>. This removes O<sub>3</sub> through chemical reaction in the absence of solar radiation. As the PBL develops in the morning, the sensitivity of O<sub>3</sub> to traffic decreases and the sensitivity to NCR emissions increases. The sensitivity to NCR emissions reaches its highest point (70%) when the PBL is fully developed around 15:00 LT. As discussed above, the downward mixing of air from the free troposphere and dilution of local emissions in the fully



developed PBL could be the reason for this. The  $O_3$  peak coincides with the highest PBL at this time because photolysis and development of the PBL are both driven by solar radiation. The development of the PBL increases the contribution from regional transport, and precursors emitted from the NCR are one of the dominant contributors to the peak of  $O_3$  in Delhi. In addition, it is noteworthy that the  $NO_x$ -rich urban plume from Delhi has a substantial influence on  $O_3$  in downwind regions across the NCR as well, as discussed in Text S3.

### 3.5 Mitigation Strategies

To demonstrate a framework for developing better mitigation strategies for addressing both  $PM_{2.5}$  and  $O_3$  pollution in Delhi, emission-sector based pollutant response surfaces are generated using Gaussian process emulation (Fig. 7). For local emissions in Delhi, we focus mainly on traffic and residential sectors here, because we find that power and industrial emissions have a more limited influence on  $PM_{2.5}$  and  $O_3$  concentrations in Delhi (Fig. 5). A range of different mitigation strategies are analysed, aiming at mitigating  $PM_{2.5}$  pollution whilst minimizing the risk of  $O_3$  increase.

We find that the responses of  $PM_{2.5}$  and  $O_3$  to each emission sector are nearly linear in Delhi. The response surfaces show that reducing local traffic emissions in Delhi leads to an efficient decrease in  $PM_{2.5}$  loading (Fig. 7a) but increases  $O_3$  greatly (Fig. 7b). Reducing local domestic emissions decreases  $PM_{2.5}$  loading less than reducing traffic but without increasing  $O_3$ . The small impact on  $O_3$  may be because domestic emissions are not a major source of  $NO_x$ , contributing only 15% of that from traffic (Fig. 6). A 10-20% reduction in  $NO_x$  is expected when reduce local domestic emissions by 50%; while, 35-45% reduction in  $NO_x$  can be expected by a 50% reduction in local traffic emissions (Fig. S7). In addition, VOC is reduced more than  $NO_x$  when controlling domestic emissions, as the VOC/ $NO_x$  emission ratio (kg/kg) is 1.8 in contrast to a ratio of 0.4 for traffic emissions. Greater reduction of VOC suppresses the increase of  $O_3$  in Delhi, which is a VOC-limited environment. A reduction in local traffic emissions alone of 50% could decrease Delhi  $PM_{2.5}$  loading by 15-20%, but this would also increase  $O_3$  by 20-25%. To prevent the side-effect of increasing  $O_3$  by controls on traffic emissions, regional cooperation would be required to reduce emissions in the NCR region surrounding Delhi by 25-30%, which also permits a



further reduction of  $PM_{2.5}$  by 5-10% (Fig. 7c and 7d). This is consistent with a recent study showing that  
345 ~60% of  $PM_{2.5}$  in Delhi originates from outside (Amann et al., 2017). The suggested regional joint  
mitigation with NCR surrounding Delhi is in line with a recent study for mitigating  $PM_{2.5}$  in Beijing,  
which showed that regional coordination over the North China Plain could lead to a reduction in  $PM_{2.5}$  of  
up to 40% in winter (Liu et al., 2016).

#### 350 4. Summary

Previous studies have shown that emission controls focusing on mitigation of  $PM_{2.5}$  may result in  
substantial increases of surface ozone over urban areas that are in VOC-limited photochemical  
environment. Comprehensive studies of mitigation strategies with respect to both  $PM_{2.5}$  and  $O_3$  are  
urgently required, but are limited in India. In this study, we demonstrate a numerical framework for  
355 informing emission-sector based mitigation strategies in Delhi that account for multiple pollutants.

By using Gaussian process emulation with an air quality model (WRF-Chem), we generate a  
computational efficient surrogate model for performing global sensitivity analysis and calculating  
emission-sector based pollutant response surfaces. These enable us to exhaustively investigate the impacts  
of different mitigation scenarios on  $PM_{2.5}$  and  $O_3$  in Delhi, which help decision makers choose better  
360 mitigation strategies. Global sensitivity analysis shows that pollutants originating from the National  
Capital Region (NCR) surrounding Delhi and local traffic emissions are the major contributors of  $PM_{2.5}$   
and  $O_3$  in Delhi. They co-dominate the  $O_3$  peak and  $PM_{2.5}$  in Delhi during daytime, while the regional  
transport governs  $PM_{2.5}$  during the night. Controlling local traffic emissions in Delhi would have the  
notable side effect of  $O_3$  increases, at least in the pre-monsoon/summer (peak  $O_3$  season) that we consider  
365 here. Our pollutant response surfaces suggest that joint coordinated emission controls with the NCR  
region surrounding Delhi would be required to minimize the risk of  $O_3$  increases and to achieve a more  
ambitious reduction of  $PM_{2.5}$ . In the regional joint coordination, residential energy use could be a  
dominant emission sector over a large region in India (Conibear et al., 2018).



## 370 5. Discussion

The experiences of developed countries (Dooley, 2002; EPA, 2011) and recently in China (Huang et al., 2018a) show that regional joint coordination can be achieved by changing energy infrastructure (e.g., replacing fossil fuel by renewable energy and natural gas), desulphurisation and denitrification technologies, popularization of new energy vehicles, strict control of vehicle exhaust and reducing road  
375 and construction dust. Further studies with more detailed information on specific emission sectors and strategies for clean-technology development and popularization would permit deeper insight into air pollution mitigation approaches suitable for Delhi. These are needed to address both PM<sub>2.5</sub> which has a higher impact on public health (e.g., Huang et al., 2018a), and O<sub>3</sub> which greatly impacts regional ecology and agriculture (e.g., Avnery et al., 2011). A more comprehensive evaluation of the health and economic  
380 benefits of different mitigation strategies would greatly help Indian decision makers, and the framework we have demonstrated here would provide a strong foundation for this.





### Author contributions

O. W. and Y. C. conceived the study. Y. C. performed the simulations and emulation, and processed and interpreted  
385 the results with help from Y. W. E. R. designed and built the Gaussian Process emulator. G. B. and S. K. S. provided the  
observations and SAFAR emission inventory. D. L., A. A., S. A.-N. and G. M. help pre-process the emission data and  
develop the emission toolkit. V. S. and R. S. S. provided useful discussion on the emission inventory. R. S. S. led the  
development of the PROMOTE project. Y. C. and O. W. wrote the manuscript with inputs from all co-authors.

### Notes

390 The authors declare no competing financial interest.

### Acknowledgments

This work was supported by the NERC/MOES/Newton Fund supported PROMOTE project (grant number  
NE/P016405/1 and NE/P016480/1). The work of E. Ryan was supported by the NERC (grant number NE/N003411/1).  
The Indian Institute of Tropical Meteorology, Pune, is supported by the Ministry of Earth Science, Government of India.  
395 The observations and high-resolution emission inventory are provided by the SAFAR project under MoES  
(<http://safar.tropmet.res.in>). The authors appreciate the efforts of the entire team involved in PROMOTE and SAFAR  
projects. The paper is based on interpretation of scientific results and in no way reflect the viewpoint of the funding  
agency.

### Data availability

400 NCEP FNL operational model global tropospheric analyses (ds083.2) were downloaded from  
<https://rda.ucar.edu/data/ds083.2/>, and sea surface temperature data were downloaded from  
<http://polar.ncep.noaa.gov/sst/>. ECMWF interim reanalyses (ERA-Interim) were downloaded from  
<http://apps.ecmwf.int/datasets/data/interim-full-daily>. MOZART-4 global model results are downloaded from  
<http://www.acd.ucar.edu/wrf-chem/mozart.shtml>. FINN biomass burning emissions dataset is downloaded from  
405 <http://bai.acom.ucar.edu/Data/fire/>. Toolkits for emission processing are available  
from [https://github.com/douglowe/WRF\\_UoM\\_EMIT/releases/tag/v1.0](https://github.com/douglowe/WRF_UoM_EMIT/releases/tag/v1.0) and [https://github.com/douglowe/PROMOTE-](https://github.com/douglowe/PROMOTE-emissions/releases/tag/v1.0)  
[emissions/releases/tag/v1.0](https://github.com/douglowe/PROMOTE-emissions/releases/tag/v1.0).



## References:

- Amann, M., Bertok, I., Borcken-Kleefeld, J., Cofala, J., Heyes, C., Höglund-Isaksson, L., Klimont, Z., Nguyen, B., Posch, M., Rafaj, P., Sandler, R., Schöpp, W., Wagner, F., and Winiwarter, W.: Cost-effective control of air quality and greenhouse gases in Europe: Modeling and policy applications, *Environmental Modelling & Software*, 26, 1489-1501, <https://doi.org/10.1016/j.envsoft.2011.07.012>, 2011.
- Amann, M., Purohit, P., Bhanarkar, A. D., Bertok, I., Borcken-Kleefeld, J., Cofala, J., Heyes, C., Kiesewetter, G., Klimont, Z., Liu, J., Majumdar, D., Nguyen, B., Rafaj, P., Rao, P. S., Sander, R., Schöpp, W., Srivastava, A., and Vardhan, B. H.: Managing future air quality in megacities: A case study for Delhi, *Atmospheric Environment*, 161, 99-111, <https://doi.org/10.1016/j.atmosenv.2017.04.041>, 2017.
- Ashworth, K., Wild, O., and Hewitt, C. N.: Impacts of biofuel cultivation on mortality and crop yields, *Nature Clim. Change*, 3, 492-496, [10.1038/nclimate1788](https://doi.org/10.1038/nclimate1788), 2013.
- Aslam, M. Y., Krishna, K. R., Beig, G., Tinmaker, M. I. R., and Chate, D. M.: Seasonal Variation of Urban Heat Island and Its Impact on Air-Quality Using SAFAR Observations at Delhi, India, *American Journal of Climate Change*, Vol.06No.02, 12, [10.4236/ajcc.2017.62015](https://doi.org/10.4236/ajcc.2017.62015), 2017.
- Avnery, S., Mauzerall, D. L., Liu, J., and Horowitz, L. W.: Global crop yield reductions due to surface ozone exposure: 2. Year 2030 potential crop production losses and economic damage under two scenarios of O<sub>3</sub> pollution, *Atmospheric Environment*, 45, 2297-2309, <https://doi.org/10.1016/j.atmosenv.2011.01.002>, 2011.
- Beig, G., Chate, D. M., Ghude, S. D., Ali, K., Satpute, T., Sahu, S. K., Parkhi, N., and Trimbake, H. K.: Evaluating population exposure to environmental pollutants during Deepavali fireworks displays using air quality measurements of the SAFAR network, *Chemosphere*, 92, 116-124, [http://dx.doi.org/10.1016/j.chemosphere.2013.02.043](https://doi.org/10.1016/j.chemosphere.2013.02.043), 2013.
- Chatani, S., and Sharma, S.: Uncertainties Caused by Major Meteorological Analysis Data Sets in Simulating Air Quality Over India, *Journal of Geophysical Research: Atmospheres*, 123, 6230-6247, [doi:10.1029/2017JD027502](https://doi.org/10.1029/2017JD027502), 2018.
- Chen, L., Guo, B., Huang, J., He, J., Wang, H., Zhang, S., and Chen, S. X.: Assessing air-quality in Beijing-Tianjin-Hebei region: The method and mixed tales of PM<sub>2.5</sub> and O<sub>3</sub>, *Atmospheric Environment*, <https://doi.org/10.1016/j.atmosenv.2018.08.047>, 2018a.
- Chen, Y., Cheng, Y., Ma, N., Wolke, R., Nordmann, S., Schüttauf, S., Ran, L., Wehner, B., Birmili, W., van der Gon, H. A. C. D., Mu, Q., Barthel, S., Spindler, G., Stieger, B., Müller, K., Zheng, G. J., Pöschl, U., Su, H., and Wiedensohler, A.: Sea salt emission, transport and influence on size-segregated nitrate simulation: a case study in northwestern Europe by WRF-Chem, *Atmos. Chem. Phys.*, 16, 12081-12097, [10.5194/acp-16-12081-2016](https://doi.org/10.5194/acp-16-12081-2016), 2016a.
- Chen, Y., Cheng, Y. F., Nordmann, S., Birmili, W., Denier van der Gon, H. A. C., Ma, N., Wolke, R., Wehner, B., Sun, J., Spindler, G., Mu, Q., Pöschl, U., Su, H., and Wiedensohler, A.: Evaluation of the size segregation of elemental carbon (EC) emission in Europe: influence on the simulation of EC long-range transportation, *Atmos. Chem. Phys.*, 16, 1823-1835, [10.5194/acp-16-1823-2016](https://doi.org/10.5194/acp-16-1823-2016), 2016b.
- Chen, Y., Wolke, R., Ran, L., Birmili, W., Spindler, G., Schröder, W., Su, H., Cheng, Y., Tegen, I., and Wiedensohler, A.: A parameterization of the heterogeneous hydrolysis of N<sub>2</sub>O<sub>5</sub> for mass-based aerosol models: improvement of particulate nitrate prediction, *Atmos. Chem. Phys.*, 18, 673-689, [10.5194/acp-18-673-2018](https://doi.org/10.5194/acp-18-673-2018), 2018b.
- Chou, M., Suarez, M., Ho, C., Yan, M., and Lee, K.: Parameterizations for Cloud Overlapping and Shortwave Single-Scattering Properties for Use in General Circulation and Cloud Ensemble, *Models, J. Climate*, 11, 202-214, 1998.
- Chowdhury, S., and Dey, S.: Cause-specific premature death from ambient PM<sub>2.5</sub> exposure in India: Estimate adjusted for baseline mortality, *Environment International*, 91, 283-290, <https://doi.org/10.1016/j.envint.2016.03.004>, 2016.
- Chowdhury, S., Dey, S., Tripathi, S. N., Beig, G., Mishra, A. K., and Sharma, S.: "Traffic intervention" policy fails to mitigate air pollution in megacity Delhi, *Environmental Science & Policy*, 74, 8-13, [http://dx.doi.org/10.1016/j.envsci.2017.04.018](https://doi.org/10.1016/j.envsci.2017.04.018), 2017.
- Conibear, L., Butt, E. W., Knote, C., Arnold, S. R., and Spracklen, D. V.: Residential energy use emissions dominate health impacts from exposure to ambient particulate matter in India, *Nature Communications*, 9, 617, [10.1038/s41467-018-02986-7](https://doi.org/10.1038/s41467-018-02986-7), 2018.
- Cusworth, D. H., Mickley, L. J., Sulprizio, M. P., Liu, T., Marlier, M. E., DeFries, R. S., Guttikunda, S. K., and Gupta, P.: Quantifying the influence of agricultural fires in northwest India on urban air pollution in Delhi, India, *Environmental Research Letters*, 13, 044018, [10.1088/1748-9326/aab303](https://doi.org/10.1088/1748-9326/aab303), 2018.
- Denier van der Gon, H. A. C., Hendriks, C., Kuenen, J., Segers, A., and Visschedijk, A.: TNO Report: Description of current temporal emission patterns and sensitivity of predicted AQ for temporal emission patterns 2011.
- Dooley, E.: Clearing the Air over the London Fog, *Environmental Health Perspectives*, 110, A748-A749, 2002.
- Duncan, B. N., Lamsal, L. N., Thompson, A. M., Yoshida, Y., Lu, Z., Streets, D. G., Hurwitz, M. M., and Pickering, K. E.: A space-based, high-resolution view of notable changes in urban NO<sub>x</sub> pollution around the world (2005–2014), *Journal of Geophysical Research: Atmospheres*, 121, 976-996, [doi:10.1002/2015JD024121](https://doi.org/10.1002/2015JD024121), 2016.



- EPA: Technical support document for the proposed PM NAAQS rule: Response Surface Modeling, Office of Air Quality Planning and Standards, US Environmental Protection Agency, Research Triangle Park, NC, US, 48, (last access: 01 Oct. 2018), 2006a.
- EPA: Technical support document for the proposed mobile source air toxics rule: ozone modeling, Office of Air Quality Planning and Standards, US Environmental Protection Agency, Research Triangle Park, NC, US, 49, (last access: 01 Oct. 2018), 2006b.
- EPA: Benefits and costs of the Clean Air Act 1990-2020, the second prospective study, <https://www.epa.gov/clean-air-act-overview/benefitsand-costs-clean-air-act-1990-2020-second-prospective-study>, (last access: 20 Aug. 2018). 2011.
- Fleming, Z. L., Doherty, R. M., Von Schneidmesser, E., Malley, C. S., Cooper, O. R., Pinto, J. P., Colette, A., Xu, X., Simpson, D., Schultz, M. G., Lefohn, A. S., Hamad, S., Moolla, R., Solberg, S., and Feng, Z.: Tropospheric Ozone Assessment Report: Present-day ozone distribution and trends relevant to human health, *Elem. Sci. Anth.*, 6, 12, 2018.
- Gao, M., Guttikunda, S. K., Carmichael, G. R., Wang, Y., Liu, Z., Stanier, C. O., Saide, P. E., and Yu, M.: Health impacts and economic losses assessment of the 2013 severe haze event in Beijing area, *Science of The Total Environment*, 511, 553-561, <https://doi.org/10.1016/j.scitotenv.2015.01.005>, 2015.
- Gao, M., Beig, G., Song, S., Zhang, H., Hu, J., Ying, Q., Liang, F., Liu, Y., Wang, H., Lu, X., Zhu, T., Carmichael, G. R., Nielsen, C. P., and McElroy, M. B.: The impact of power generation emissions on ambient PM<sub>2.5</sub> pollution and human health in China and India, *Environment International*, 121, 250-259, <https://doi.org/10.1016/j.envint.2018.09.015>, 2018.
- Ghude, S. D., Jain, S. L., Arya, B. C., Beig, G., Ahammed, Y. N., Kumar, A., and Tyagi, B.: Ozone in ambient air at a tropical megacity, Delhi: characteristics, trends and cumulative ozone exposure indices, *J Atmos Chem*, 60, 237-252, 10.1007/s10874-009-9119-4, 2008.
- Ghude, S. D., Jena, C., Chate, D. M., Beig, G., Pfister, G. G., Kumar, R., and Ramanathan, V.: Reductions in India's crop yield due to ozone, *Geophysical Research Letters*, 41, 5685-5691, 10.1002/2014GL060930, 2014.
- Ghude, S. D., Chate, D. M., Jena, C., Beig, G., Kumar, R., Barth, M. C., Pfister, G. G., Fadnavis, S., and Pithani, P.: Premature mortality in India due to PM<sub>2.5</sub> and ozone exposure, *Geophysical Research Letters*, 43, 4650-4658, 10.1002/2016GL068949, 2016.
- Grell, G. A., Peckham, S. E., Schmitz, R., McKeen, S. A., Frost, G., Skamarock, W. C., and Eder, B.: Fully coupled "online" chemistry within the WRF model, *Atmospheric Environment*, 39, 6957-6975, <http://dx.doi.org/10.1016/j.atmosenv.2005.04.027>, 2005.
- Guenther, A., Karl, T., Harley, P., Wiedinmyer, C., Palmer, P. I., and Geron, C.: Estimates of global terrestrial isoprene emissions using MEGAN (Model of Emissions of Gases and Aerosols from Nature), *Atmos. Chem. Phys.*, 6, 3181-3210, 10.5194/acp-6-3181-2006, 2006.
- Gupta, M., and Mohan, M.: Validation of WRF/Chem model and sensitivity of chemical mechanisms to ozone simulation over megacity Delhi, *Atmospheric Environment*, 122, 220-229, <http://dx.doi.org/10.1016/j.atmosenv.2015.09.039>, 2015.
- Hollaway, M., Wild, O., Yang, T., Sun, Y., Xu, W., Xie, C., Whalley, L., Slater, E., Heard, D., and Liu, D.: Photochemical impacts of haze pollution in an urban environment, *Atmos. Chem. Phys. Discuss.*, 2019, 1-26, 10.5194/acp-2019-29, 2019.
- Hong, S.-Y., Noh, Y., and Dudhia, J.: A new vertical diffusion package with an explicit treatment of entrainment processes, *Mon. Weather Rev.*, 134, 2318-2341, 2006.
- Hu, D., Chen, Y., Wang, Y., Daële, V., Idir, M., Yu, C., Wang, J., and Mellouki, A.: Photochemical reaction playing a key role in particulate matter pollution over Central France: Insight from the aerosol optical properties, *Science of The Total Environment*, 657, 1074-1084, <https://doi.org/10.1016/j.scitotenv.2018.12.084>, 2019.
- Huang, G., Brook, R., Crippa, M., Janssens-Maenhout, G., Schieberle, C., Dore, C., Guizzardi, D., Muntean, M., Schaaf, E., and Friedrich, R.: Speciation of anthropogenic emissions of non-methane volatile organic compounds: a global gridded data set for 1970-2012, *Atmos. Chem. Phys.*, 17, 7683-7701, 10.5194/acp-17-7683-2017, 2017.
- Huang, J., Pan, X., Guo, X., and Li, G.: Health impact of China's Air Pollution Prevention and Control Action Plan: an analysis of national air quality monitoring and mortality data, *The Lancet Planetary Health*, 2, e313-e323, 10.1016/S2542-5196(18)30141-4, 2018a.
- Huang, X., Wang, Z., and Ding, A.: Impact of Aerosol-PBL Interaction on Haze Pollution: Multiyear Observational Evidences in North China, *Geophysical Research Letters*, 45, 8596-8603, 10.1029/2018GL079239, 2018b.
- Iooss, B., and Lemaître, P.: A review on global sensitivity analysis methods. In: Meloni, C., Dellino, G. (Eds.), *Uncertainty Management in Simulation Optimization of Complex Systems: Algorithms and Applications*. Springer, 2015.
- Janssens-Maenhout, G., Crippa, M., Guizzardi, D., Dentener, F., Muntean, M., Pouliot, G., Keating, T., Zhang, Q., Kurokawa, J., Wankmüller, R., Denier van der Gon, H., Kuenen, J. J. P., Klimont, Z., Frost, G., Darras, S., Koffi, B., and Li, M.:



- HTAP\_v2.2: a mosaic of regional and global emission grid maps for 2008 and 2010 to study hemispheric transport of air pollution, *Atmos. Chem. Phys.*, 15, 11411-11432, 10.5194/acp-15-11411-2015, 2015.
- Jethva, H., Chand, D., Torres, O., Gupta, P., Lyapustin, A., and Patadia, F.: Agricultural Burning and Air Quality over Northern India: A Synergistic Analysis using NASA's A-train Satellite Data and Ground Measurements, *Aerosol and Air Quality Research*, 18, 1756-1773, 10.4209/aaqr.2017.12.0583, 2018.
- Khare, M., Gargava, P., and Khan, A. A.: Effect of PM<sub>2.5</sub> chemical constituents on atmospheric visibility impairment AU - Khanna, Isha, *Journal of the Air & Waste Management Association*, 68, 430-437, 10.1080/10962247.2018.1425772, 2018.
- Kumar, R., Barth, M. C., Madronich, S., Naja, M., Carmichael, G. R., Pfister, G. G., Knote, C., Brasseur, G. P., Ojha, N., and Sarangi, T.: Effects of dust aerosols on tropospheric chemistry during a typical pre-monsoon season dust storm in northern India, *Atmos. Chem. Phys.*, 14, 6813-6834, 10.5194/acp-14-6813-2014, 2014a.
- Kumar, R., Barth, M. C., Pfister, G. G., Naja, M., and Brasseur, G. P.: WRF-Chem simulations of a typical pre-monsoon dust storm in northern India: influences on aerosol optical properties and radiation budget, *Atmos. Chem. Phys.*, 14, 2431-2446, 10.5194/acp-14-2431-2014, 2014b.
- Kumar, R., Barth, M. C., Pfister, G. G., Delle Monache, L., Lamarque, J. F., Archer-Nicholls, S., Tilmes, S., Ghude, S. D., Wiedinmyer, C., Naja, M., and Walters, S.: How Will Air Quality Change in South Asia by 2050?, *Journal of Geophysical Research: Atmospheres*, 123, 1840-1864, doi:10.1002/2017JD027357, 2018.
- Lee, L. A., Carslaw, K. S., Pringle, K. J., Mann, G. W., and Spracklen, D. V.: Emulation of a complex global aerosol model to quantify sensitivity to uncertain parameters, *Atmos. Chem. Phys.*, 11, 12253-12273, 10.5194/acp-11-12253-2011, 2011.
- Lee, L. A., Carslaw, K. S., Pringle, K. J., and Mann, G. W.: Mapping the uncertainty in global CCN using emulation, *Atmos. Chem. Phys.*, 12, 9739-9751, 10.5194/acp-12-9739-2012, 2012.
- Lee, L. A., Reddington, C. L., and Carslaw, K. S.: On the relationship between aerosol model uncertainty and radiative forcing uncertainty, *Proceedings of the National Academy of Sciences*, 113, 5820-5827, 10.1073/pnas.1507050113, 2016.
- Lelieveld, J., Bourtsoukidis, E., Brühl, C., Fischer, H., Fuchs, H., Harder, H., Hofzumahaus, A., Holland, F., Marno, D., Neumaier, M., Pozzer, A., Schlager, H., Williams, J., Zahn, A., and Ziereis, H.: The South Asian monsoon—Pollution pump and purifier, *Science*, 10.1126/science.aar2501, 2018.
- Li, K., Jacob, D. J., Liao, H., Shen, L., Zhang, Q., and Bates, K. H.: Anthropogenic drivers of 2013–2017 trends in summer surface ozone in China, *Proceedings of the National Academy of Sciences*, 201812168, 10.1073/pnas.1812168116, 2018.
- Lin, Y., Farley, R., and Orville, H.: Bulk Parameterization of the Snow Field in a Cloud Model, *J. Clim. Appl. Meteorol.*, 22, 1065-1092, 1983.
- Liu, H., Wang, X. M., Pang, J. M., and He, K. B.: Feasibility and difficulties of China's new air quality standard compliance: PRD case of PM<sub>2.5</sub> and ozone from 2010 to 2025, *Atmos. Chem. Phys.*, 13, 12013-12027, 10.5194/acp-13-12013-2013, 2013.
- Liu, J., Mauzerall, D. L., Chen, Q., Zhang, Q., Song, Y., Peng, W., Klimont, Z., Qiu, X., Zhang, S., Hu, M., Lin, W., Smith, K. R., and Zhu, T.: Air pollutant emissions from Chinese households: A major and underappreciated ambient pollution source, *Proceedings of the National Academy of Sciences*, 113, 7756-7761, 10.1073/pnas.1604537113, 2016.
- Liu, J., Xiang, S., Yi, K., and Tao, W.: Co-Mitigation of Ozone and PM<sub>2.5</sub> Pollution over the Beijing-Tianjin-Hebei Region, 2017 AGU Fall Meeting, New Orleans, 2017AGUFM.A53F2327L, 2017.
- Lu, X., Hong, J., Zhang, L., Cooper, O. R., Schultz, M. G., Xu, X., Wang, T., Gao, M., Zhao, Y., and Zhang, Y.: Severe Surface Ozone Pollution in China: A Global Perspective, *Environmental Science & Technology Letters*, 10.1021/acs.estlett.8b00366, 2018.
- Marrapu, P., Cheng, Y., Beig, G., Sahu, S., Srinivas, R., and Carmichael, G. R.: Air quality in Delhi during the Commonwealth Games, *Atmos. Chem. Phys.*, 14, 10619-10630, 10.5194/acp-14-10619-2014, 2014.
- Mohan, M., and Bhati, S.: Analysis of WRF Model Performance over Subtropical Region of Delhi, India, *Advances in Meteorology*, 2011, 10.1155/2011/621235, 2011.
- Mohan, M., and Gupta, M.: Sensitivity of PBL parameterizations on PM<sub>10</sub> and ozone simulation using chemical transport model WRF-Chem over a sub-tropical urban airshed in India, *Atmospheric Environment*, 185, 53-63, <https://doi.org/10.1016/j.atmosenv.2018.04.054>, 2018.
- Mukherjee, A., and Toohey, D. W.: A study of aerosol properties based on observations of particulate matter from the U.S. Embassy in Beijing, China, *Earth's Future*, 4, 381-395, doi:10.1002/2016EF000367, 2016.
- Murrells, T. P., Passant, N. R., Thistlethwaite, G., Wagner, A., Li, Y., Bush, T., Norris, J., Walker, C., Stewart, R. A., Tsagatakis, I., Whiting, R., Conolly, C., Okamura, S., Peirce, M., Sneddon, S., Webb, J., Thomas, J., MacCarthy, J., Choudrie, S., Webb, N., and Mould, R.: UK Emissions of Air Pollutants 1970 to 2009, Available: [20](https://uk-</a></p></div><div data-bbox=)



air.defra.gov.uk/assets/documents/reports/cat07/1401131501\_NAEI\_Annual\_Report\_2009.pdf, (last access: 12 Nov. 2018), 2009.

- O'Hagan, A.: Bayesian analysis of computer code outputs: A tutorial, *Reliability Engineering & System Safety*, 91, 1290-1300, <https://doi.org/10.1016/j.res.2005.11.025>, 2006.
- O'Hagan, A., and West, M.: *Handbook of applied Bayesian analysis*, Oxford University Press, New York, 2009.
- Ojha, N., Naja, M., Singh, K. P., Sarangi, T., Kumar, R., Lal, S., Lawrence, M. G., Butler, T. M., and Chandola, H. C.: Variabilities in ozone at a semi-urban site in the Indo-Gangetic Plain region: Association with the meteorology and regional processes, *Journal of Geophysical Research: Atmospheres*, 117, doi:10.1029/2012JD017716, 2012.
- Pisoni, E., Clappier, A., Degraeuwe, B., and Thunis, P.: Adding spatial flexibility to source-receptor relationships for air quality modeling, *Environmental Modelling & Software*, 90, 68-77, <https://doi.org/10.1016/j.envsoft.2017.01.001>, 2017.
- Pisoni, E., Albrecht, D., Mara, T. A., Rosati, R., Tarantola, S., and Thunis, P.: Application of uncertainty and sensitivity analysis to the air quality SHERPA modelling tool, *Atmospheric Environment*, 183, 84-93, <https://doi.org/10.1016/j.atmosenv.2018.04.006>, 2018.
- Pope, C. A., Ezzati, M., and Dockery, D. W.: Fine-Particulate Air Pollution and Life Expectancy in the United States, *New England Journal of Medicine*, 360, 376-386, 10.1056/NEJMsa0805646, 2009.
- Ran, L., Zhao, C., Geng, F., Tie, X., Tang, X., Peng, L., Zhou, G., Yu, Q., Xu, J., and Guenther, A.: Ozone photochemical production in urban Shanghai, China: Analysis based on ground level observations, *Journal of Geophysical Research: Atmospheres*, 114, D15301, 10.1029/2008JD010752, 2009.
- Ryan, E., Wild, O., Voulgarakis, A., and Lee, L.: Fast sensitivity analysis methods for computationally expensive models with multi-dimensional output, *Geosci. Model Dev.*, 11, 3131-3146, 10.5194/gmd-11-3131-2018, 2018.
- Sahu, S. K., Beig, G., and Parkhi, N. S.: Emissions inventory of anthropogenic PM<sub>2.5</sub> and PM<sub>10</sub> in Delhi during Commonwealth Games 2010, *Atmospheric Environment*, 45, 6180-6190, <http://dx.doi.org/10.1016/j.atmosenv.2011.08.014>, 2011.
- Sahu, S. K., Beig, G., and Parkhi, N.: High Resolution Emission Inventory of NO<sub>x</sub> and CO for Mega City Delhi, India, *Aerosol and Air Quality Research*, 15, 1137-1144, 10.4209/aaqr.2014.07.0132, 2015.
- Saltelli, A., Tarantola, S., and Chan, K. P. S.: A Quantitative Model-Independent Method for Global Sensitivity Analysis of Model Output, *Technometrics*, 41, 39-56, 10.1080/00401706.1999.10485594, 1999.
- Sharma, A., Ojha, N., Pozzer, A., Mar, K. A., Beig, G., Lelieveld, J., and Gunthe, S. S.: WRF-Chem simulated surface ozone over south Asia during the pre-monsoon: effects of emission inventories and chemical mechanisms, *Atmos. Chem. Phys.*, 17, 14393-14413, 10.5194/acp-17-14393-2017, 2017.
- Sharma, S. K., Mandal, T. K., Sharma, A., Jain, S., and Saraswati: Carbonaceous Species of PM<sub>2.5</sub> in Megacity Delhi, India During 2012–2016, *Bulletin of Environmental Contamination and Toxicology*, 100, 695-701, 10.1007/s00128-018-2313-9, 2018.
- Shields, M. D., and Zhang, J.: The generalization of Latin hypercube sampling, *Reliability Engineering & System Safety*, 148, 96-108, <https://doi.org/10.1016/j.res.2015.12.002>, 2016.
- Stafoggia, M., Bellander, T., Bucci, S., Davoli, M., de Hoogh, K., de Donato, F., Gariazzo, C., Lyapustin, A., Michelozzi, P., Renzi, M., Scortichini, M., Shtein, A., Viegi, G., Kloog, I., and Schwartz, J.: Estimation of daily PM<sub>10</sub> and PM<sub>2.5</sub> concentrations in Italy, 2013–2015, using a spatiotemporal land-use random-forest model, *Environment International*, 124, 170-179, <https://doi.org/10.1016/j.envint.2019.01.016>, 2019.
- Thunis, P., Degraeuwe, B., Pisoni, E., Ferrari, F., and Clappier, A.: On the design and assessment of regional air quality plans: The SHERPA approach, *Journal of Environmental Management*, 183, 952-958, <https://doi.org/10.1016/j.jenvman.2016.09.049>, 2016.
- Tie, X., Huang, R.-J., Cao, J., Zhang, Q., Cheng, Y., Su, H., Chang, D., Pöschl, U., Hoffmann, T., Dusek, U., Li, G., Worsnop, D. R., and O'Dowd, C. D.: Severe Pollution in China Amplified by Atmospheric Moisture, *Scientific Reports*, 7, 15760, 10.1038/s41598-017-15909-1, 2017.
- Turner, M. C., Jerrett, M., Pope, C. A., 3rd, Krewski, D., Gapstur, S. M., Diver, W. R., Beckerman, B. S., Marshall, J. D., Su, J., Crouse, D. L., and Burnett, R. T.: Long-Term Ozone Exposure and Mortality in a Large Prospective Study, *American journal of respiratory and critical care medicine*, 193, 1134-1142, 10.1164/rccm.201508-1633OC, 2016.
- Wang, S., Xing, J., Jang, C., Zhu, Y., Fu, J. S., and Hao, J.: Impact Assessment of Ammonia Emissions on Inorganic Aerosols in East China Using Response Surface Modeling Technique, *Environmental Science & Technology*, 45, 9293-9300, 10.1021/es2022347, 2011.
- Wang, T., Xue, L., Brimblecombe, P., Lam, Y. F., Li, L., and Zhang, L.: Ozone pollution in China: A review of concentrations, meteorological influences, chemical precursors, and effects, *Science of The Total Environment*, 575, 1582-1596, <https://doi.org/10.1016/j.scitotenv.2016.10.081>, 2017.



- Wang, Y., and Chen, Y.: Significant Climate Impact of Highly Hygroscopic Atmospheric Aerosols in Delhi, India, *Geophysical Research Letters*, 0, 10.1029/2019GL082339, 2019.
- WHO: Review of evidence on health aspects of air pollution - REVIHAAP final technical report, World Health Organization: Geneva, 2013.
- WHO: WHO Global Urban Ambient Air Pollution Database (update 2016), Available: <http://www.who.int/airpollution/data/cities-2016/en/>, (last access: 08 Nov. 2018), 2016a.
- WHO: Neurological syndrome and congenital anomalies, Zika Situation Report, 1-7, 2016b.
- Wiedinmyer, C., Akagi, S. K., Yokelson, R. J., Emmons, L. K., Al-Saadi, J. A., Orlando, J. J., and Soja, A. J.: The Fire INventory from NCAR (FINN): a high resolution global model to estimate the emissions from open burning, *Geosci. Model Dev.*, 4, 625-641, 10.5194/gmd-4-625-2011, 2011.
- Wild, O., Zhu, X., and Prather, M. J.: Fast-J: Accurate Simulation of In- and Below-Cloud Photolysis in Tropospheric Chemical Models, *J. Atmos. Chem.*, 37, 245-282, 2000.
- Willmott, C. J., Robeson, S. M., and Matsuura, K.: A refined index of model performance, *International Journal of Climatology*, 32, 2088-2094, doi:10.1002/joc.2419, 2012.
- Wu, J., Xu, Y., and Zhang, B.: Projection of PM<sub>2.5</sub> and Ozone Concentration Changes over the Jing-Jin-Ji Region in China, 143-146 pp., 2015.
- Wu, Z., Wang, Y., Tan, T., Zhu, Y., Li, M., Shang, D., Wang, H., Lu, K., Guo, S., Zeng, L., and Zhang, Y.: Aerosol Liquid Water Driven by Anthropogenic Inorganic Salts: Implying Its Key Role in Haze Formation over the North China Plain, *Environmental Science & Technology Letters*, 5, 160-166, 10.1021/acs.estlett.8b00021, 2018.
- Xing, J., Wang, S., Zhao, B., Wu, W., Ding, D., Jang, C., Zhu, Y., Chang, X., Wang, J., Zhang, F., and Hao, J.: Quantifying Nonlinear Multiregional Contributions to Ozone and Fine Particles Using an Updated Response Surface Modeling Technique, *Environmental Science & Technology*, 51, 11788-11798, 10.1021/acs.est.7b01975, 2017.
- Xing, J., Ding, D., Wang, S., Zhao, B., Jang, C., Wu, W., Zhang, F., Zhu, Y., and Hao, J.: Quantification of the enhanced effectiveness of NO<sub>x</sub> control from simultaneous reductions of VOC and NH<sub>3</sub> for reducing air pollution in the Beijing–Tianjin–Hebei region, China, *Atmos. Chem. Phys.*, 18, 7799-7814, 10.5194/acp-18-7799-2018, 2018.
- Zaveri, R. A., and Peters, L. K.: A new lumped structure photochemical mechanism for large-scale applications, *J. Geophys. Res.*, 104, 30387-30415, 1999.
- Zaveri, R. A., Easter, R. C., Fast, J. D., and Peters, L. K.: Model for Simulating Aerosol Interactions and Chemistry (MOSAIC), *Journal of Geophysical Research: Atmospheres*, 113, 10.1029/2007JD008782, 2008.
- Zhao, B., Wu, W., Wang, S., Xing, J., Chang, X., Liou, K. N., Jiang, J. H., Gu, Y., Jang, C., Fu, J. S., Zhu, Y., Wang, J., Lin, Y., and Hao, J.: A modeling study of the nonlinear response of fine particles to air pollutant emissions in the Beijing–Tianjin–Hebei region, *Atmos. Chem. Phys.*, 17, 12031-12050, 10.5194/acp-17-12031-2017, 2017.
- Zhu, T., Shang, J., and Zhao, D.: The roles of heterogeneous chemical processes in the formation of an air pollution complex and gray haze, *Science China Chemistry*, 54, 145-153, 10.1007/s11426-010-4181-y, 2011.



**Table 1.** Configuration of WRF-Chem

<b>Physics</b>	<b>WRF option</b>
Micro physics	Lin scheme (Lin, 1983)
Surface Layer	MM5 similarity
Boundary layer	YSU (Hong, 2006)
Cumulus	Grell 3D
Urban	3-category UCM
Shortwave radiation	Goddard shortwave (Chou, 1998)
Longwave radiation	Rapid Radiative Transfer Model
<b>Chemistry and Aerosol</b>	<b>Chem option</b>
Gas-phase mechanism	CBMZ (Zaveri and Peters, 1999)
Aerosol module	MOSAIC with 4 bins (~40 nm to 10 μm) (Zaveri et al., 2008)
Photolysis rate	Fast-J photolysis scheme (Wild et al., 2000)
<b>Emissions Inventories</b>	
Anthropogenic Emissions	SAFAR-2015 Delhi and EDGAR-HTAP v2.2
Biogenic Emissions	MEGAN (Guenther et al., 2006)
Biomass Burning Emissions	FINN (Wiedinmyer et al., 2011)



**Table 2.** Map of NMVOC from EDGAR emission to CBMZ scheme.

EDGAR Name	Description	CBMZ [mol]
VOC1	Alcohols	20% CH <sub>3</sub> OH 80% C <sub>2</sub> H <sub>5</sub> OH
VOC2	Ethane	C <sub>2</sub> H <sub>6</sub>
VOC3	Propane	PAR*3
VOC4	Butane	PAR*4
VOC5	Pentane	PAR*5
VOC6	Hexanes + other Alkanes	PAR*6
VOC7	Ethene	ETH
VOC8	Propene	OLET+PAR
VOC9	Ethyne	PAR*2
VOC10	Isoprene	ISOP
VOC11	Monoterpenes	ISOP*2
VOC12	Other Alkenes	OLEI*0.5+OLET*0.5+PAR*2
VOC13	Benzene	TOL-PAR
VOC14	Toluene	TOL
VOC15	Xylenes	XYL
VOC16	Trimethylbenzenes	XYL+PAR
VOC17	Other Aromatics	XYL+PAR
VOC18	Esters	RCOOH
VOC19	Ethers	20% CH <sub>3</sub> OH 80% C <sub>2</sub> H <sub>5</sub> OH
VOC21	Formaldehyde	HCHO
VOC22	Other Aldehydes	ALD2
VOC23	Ketones	60% KET 40% KET+PAR
VOC24	Alkanoic Acids	RCOOH



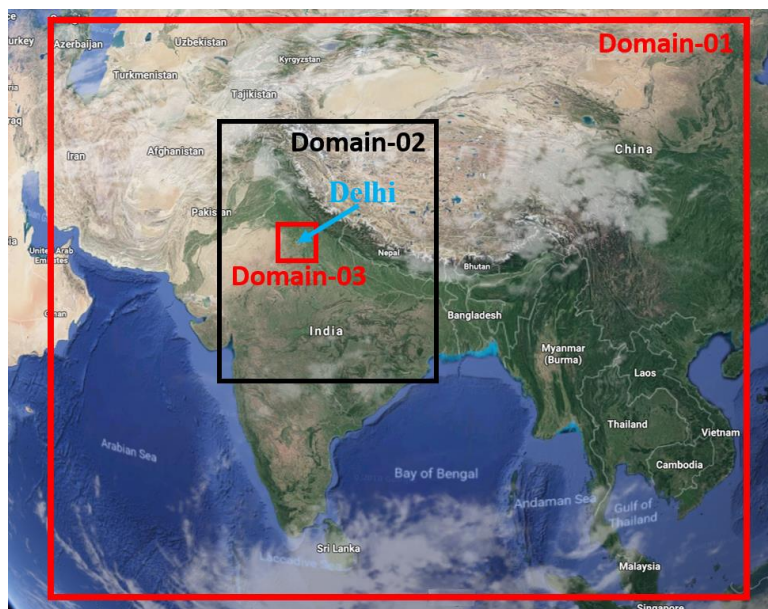


Figure 1. Map of simulation domains, modified from © Google Earth.

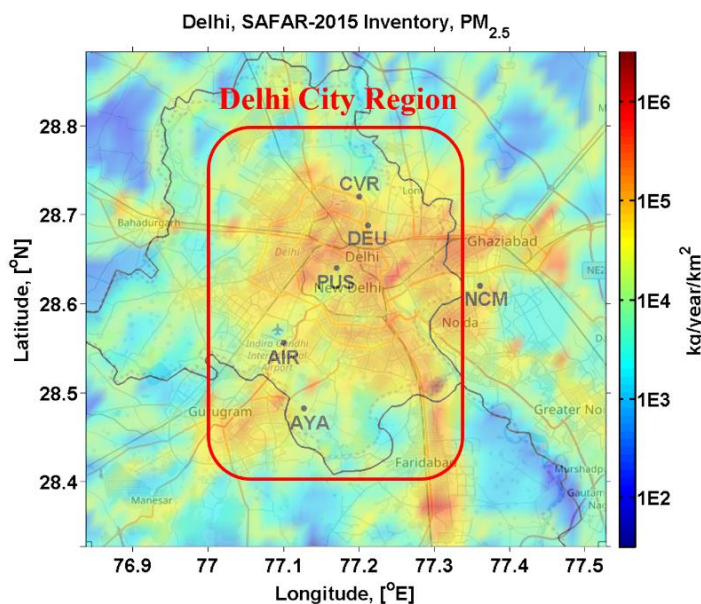
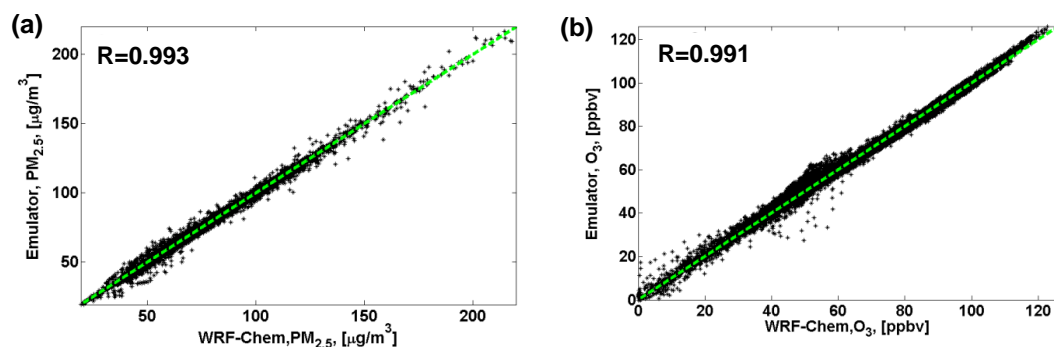
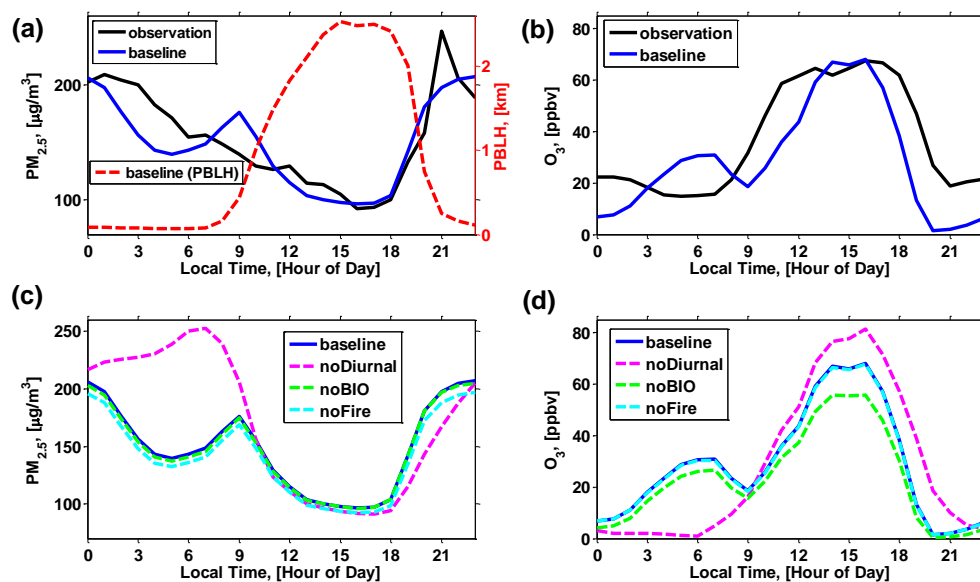


Figure 2. SAFAR inventory of total  $PM_{2.5}$  emission. The locations of measurement sites over Delhi are marked by black dots, and the Delhi City Region is marked by a red box.



**Figure 3.** Validation of Gaussian process emulator with WRF-Chem model. (a)  $PM_{2.5}$ ; (b)  $O_3$ . The green dashed line indicates the 1:1 line.



**Figure 4.** Average diurnal patterns of pollutants during the 2-15 May 2015 simulation period. (a) Modelled and observed  $PM_{2.5}$  and model PBL height (PBLH); (b)  $O_3$ ; (c) results of sensitivity studies for  $PM_{2.5}$ ; (d) results of sensitivity studies for  $O_3$ . The left panels (a, c) are for site CVR, and the right panels (b, d) are for site AIR (marked in Fig. 2). The sensitivity runs ‘noFire’ and ‘noBIO’ show model results without biomass burning and biogenic emissions, respectively; and ‘noDiurnal’ show model results with constant anthropogenic emissions rates throughout the day.

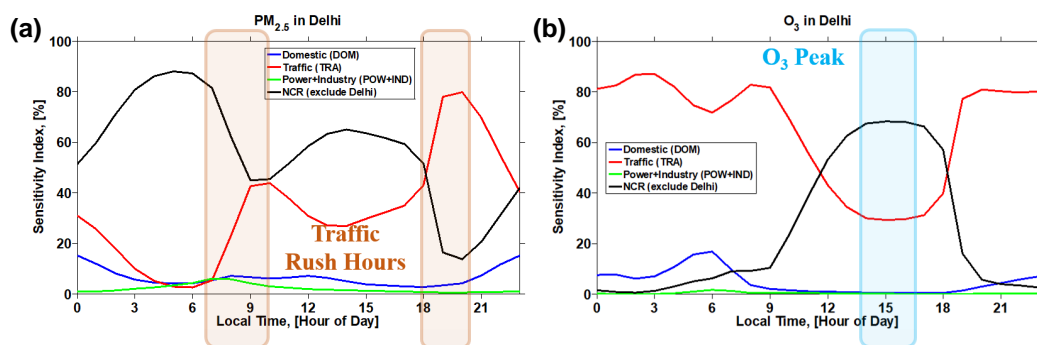


**Figure 5.** Averaged diurnal pattern of global sensitivity indices during the 2-15 May simulation period. (a) PM<sub>2.5</sub>; (b) O<sub>3</sub>. The PM<sub>2.5</sub> and O<sub>3</sub> results are averaged over Delhi City Region (marked with red box in Fig. 2). The morning and evening rush hours and the period of peak ozone are marked with the boxes to highlight the notable changes in contribution from each emission sector.

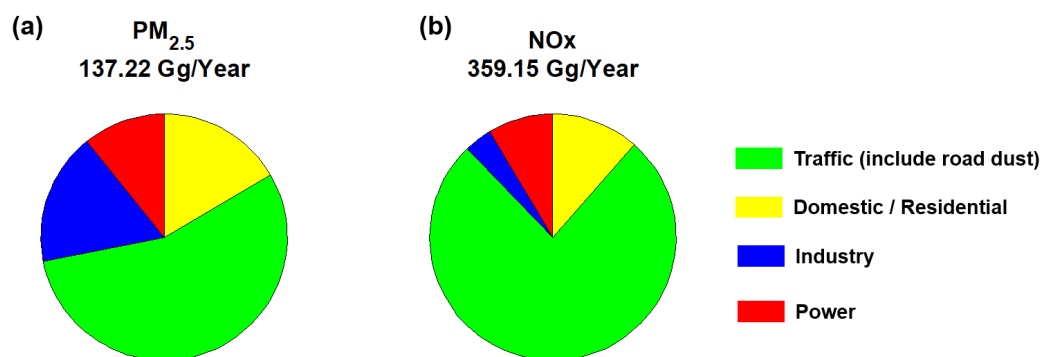


**Figure 6.** Annual emission of different sectors in Delhi from SAFAR inventory. (a) PM<sub>2.5</sub>; (b) NO<sub>x</sub>.

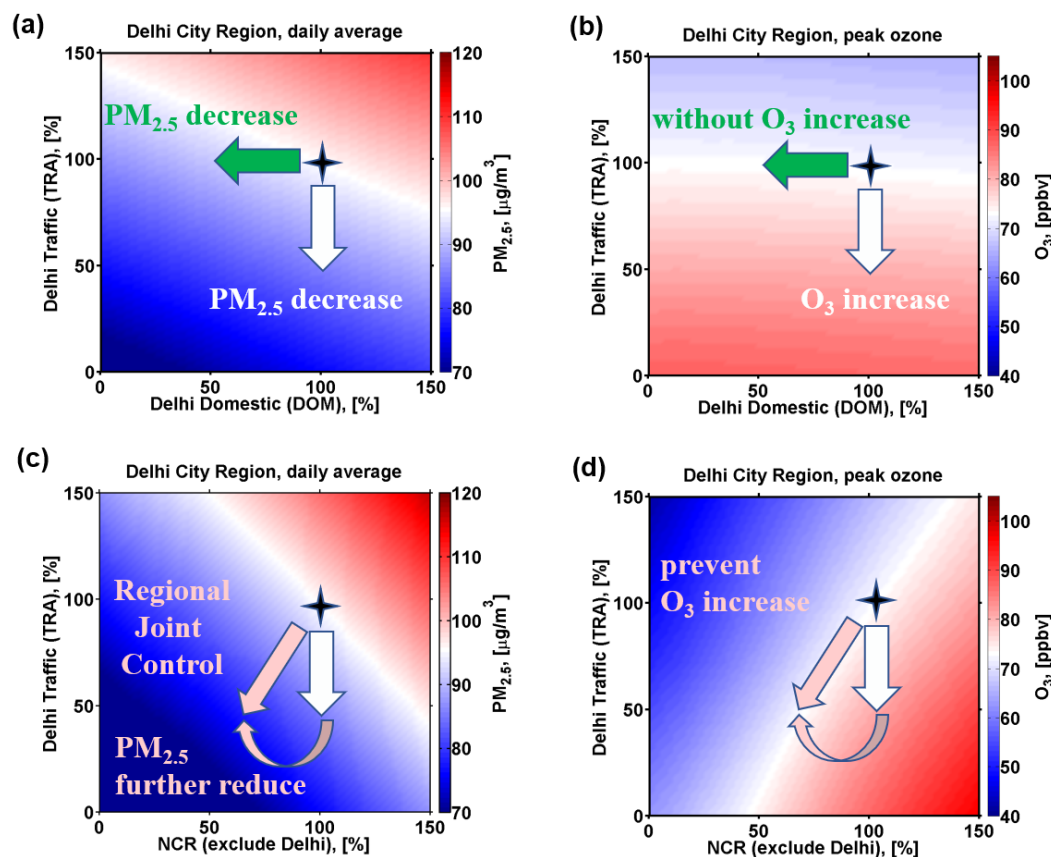


**Figure 7.** Response surfaces for PM<sub>2.5</sub> and ozone concentrations over Delhi City Region, averaged over 2-15 May 2018. (a) Daily average of PM<sub>2.5</sub> concentrations as a function of local traffic and domestic emissions in Delhi; (b) peak hourly ozone concentrations as a function of local traffic and domestic emissions in Delhi; (c) daily average of PM<sub>2.5</sub> concentrations as a function of local traffic emissions in Delhi and emissions in NCR region surrounding Delhi; and (d) peak hourly ozone concentrations as a function of local traffic emissions in Delhi and emissions in NCR region surrounding Delhi. The star indicates current conditions and the arrows show the effect of possible emission controls.